Editors' Suggestion

Enantioselective One-Photon Excitation of Formic Acid

D. Tsitsonis,[1] F. Trinter,[2] J. B. Williams,[3] K. Fehre,[1] Ph. V. Demekhin,[4,*] T. Jahnke,[5,6] R. Dörner,[1,†] and M. S. Schöffler[1,‡]

[1]*Institut für Kernphysik, Goethe-Universität Frankfurt, Max-von-Laue-Straße 1, 60438 Frankfurt am Main, Germany*
[2]*Molecular Physics, Fritz-Haber-Institut der Max-Planck-Gesellschaft, Faradayweg 4-6, 14195 Berlin, Germany*
[3]*Department of Physics, University of Nevada, Reno, Nevada 89557, USA*
[4]*Institut für Physik und CINSaT, Universität Kassel, Heinrich-Plett-Straße 40, 34132 Kassel, Germany*
[5]*Max-Planck-Institut für Kernphysik, Saupfercheckweg 1, 69117 Heidelberg, Germany*
[6]*European XFEL, Holzkoppel 4, 22869 Schenefeld, Germany*

(Received 23 March 2024; accepted 5 August 2024; published 29 August 2024)

We use one-photon excitation to promote K-shell electrons of formic acid (which has a planar equilibrium structure) to an antibonding π^* orbital. The excited molecule is known to have a (chiral) pyramidal equilibrium structure. In our experiment, we determine the handedness of the excited molecule by imaging the momenta of charged fragments, which occur after its Coulomb explosion triggered by Auger-Meitner decay cascades succeeding the excitation. We find that the handedness of the excited molecule depends on its spatial orientation with respect to the propagation (or polarization) direction of the exciting photon. The effect is largely independent of the exact polarization properties of the light driving the $1s \rightarrow \pi^*$ excitation.

DOI: 10.1103/PhysRevLett.133.093002

Many molecules with three-dimensional structure are chiral, i.e., they exist in two enantiomeric configurations that are mirror images of each other. Neglecting a tiny effect of the weak interaction, the two enantiomers of these molecules have identical energy eigenvalues. Thus, when generating chiral molecules from achiral precursors or for sorting chiral molecules from racemic ensembles, energy alone is not a sufficient control parameter to generate enantiomeric excess. To reach this goal of enhancing the population of one enantiomer over the other, usually reagents are used that are chiral themselves. Light can serve as such a reagent [1] and coherent-control schemes have been suggested in the past to synthesize or sort enantiomers [1–5]. Here, we show experimentally that even one photon with an energy, which is resonant with an internal transition in the molecule, can efficiently direct the formation of chiral molecular structure from an achiral precursor achieving enantiomeric excess. Earlier, chiral and enantioselective fragmentation of formic acid (HCOOH) has also been observed in strong laser fields [6]. However, given the extreme conditions of strong-field ionization and the many sequential steps of multiple ionization and excitation, it remained unclear which part of the complex ionization process caused the chiral effect in the end. Our present study employs high-energy photons for the one-photon ionization, which allows one to finally inspect the process in a well controlled and transparent manner, yielding a clear quantum mechanical explanation of the mechanism.

To this end, we study photoexcitation of formic acid, a molecule that has a planar prochiral equilibrium structure in its electronic ground state. Electronically excited states with an electron in the LUMO π^* orbital, however, have a three-dimensional chiral equilibrium structure and thus exist in two enantiomeric forms [7–9]. We populate this antibonding orbital by one-photon excitation of an electron from the K shell of the carbon atom or one of the two oxygen atoms at their respective resonant transition energies of 288.2 eV (C 1s), 532.1 eV [O 1s (C═O)], and 535.3 eV [O 1s (C─OH)] [10]. For comparison, we also performed the same experiment at photon energies where a σ^* state is excited, which is known to have a planar equilibrium structure. Corresponding energies are 292.0 eV [C 1s 3s/σ^*(HCO)], 296.1 eV [C 1s σ^*(C─OH)], and 303.0 eV [C 1s σ^*(C═O)] [10]. The inner-shell-excited neutral molecule de-excites by a single Auger-Meitner decay or by Auger-Meitner cascades on a timescale of a

*Contact author: demekhin@physik.uni-kassel.de
†Contact author: doerner@atom.uni-frankfurt.de
‡Contact author: schoeffler@atom.uni-frankfurt.de

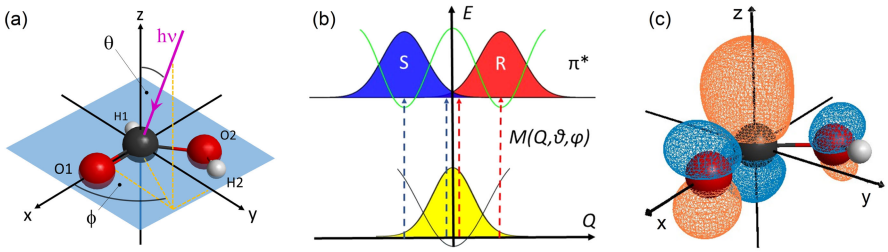

FIG. 1. Schematic representations of the experimental geometry and the considered molecular excitation process. (a) Definition of angles from which the photon approaches the formic acid molecule in its prochiral ground state (i.e., planar structure). The polar angle θ is the angle between the photon direction and the normal to the O1═C─O2 plane. The azimuthal angle ϕ is defined with respect to the C═O1 bond. (b) Sketch of the potential energy surfaces involved in the excitation. Horizontal axis: generalized bending coordinate of formic acid, $Q = 0$ corresponds to the planar configuration, $Q > 0$ to the R geometry, and $Q < 0$ to the S geometry. The lowest potential energy surface shows the electronic ground state and the upper double-well surface shows the π^* state with S or R equilibrium configuration. The dashed arrows indicate the electronic excitation. The excitation matrix element $M(Q, \theta, \phi)$ depends for each configuration Q differently on the light propagation direction in the molecular frame of reference as defined by the angles θ and ϕ. (c) The π^* orbital for a chiral geometry in which the H2 atom is bent by $Q = +20°$ out of plane. The positive (negative) phase of the orbital is encoded in the orange (cyan) color.

few femtoseconds. The latter can lead to the creation of three or more charges and a Coulomb explosion of the molecule. When more than three molecular fragments are formed, their momentum vectors are not necessarily coplanar and the handedness of the molecule prior to the fragmentation can be inferred from the fragment momenta (see, e.g., Refs. [6,11,12]).

We carried out several experiments employing different light sources and polarization properties of the exciting photons. Experiments using circularly polarized light were performed at beamline P04 of the synchrotron radiation facility PETRA III at DESY (Hamburg, Germany) in 40-bunch mode [13]. The experiment using linearly polarized light was performed at beamline SEXTANTS at synchrotron SOLEIL in 8-bunch mode [14]. In both cases, the pulsed photon beam was crossed with a supersonic molecular beam [15] in a COLTRIMS reaction microscope [16–18]. Electrons and ions were guided by an electric field of 160 V/cm onto microchannel-plate detectors with hexagonal delay-line position readout [19]. The detected electrons were only used to tag the photon bunch initiating the excitation, all other information provided by the detected electrons was discarded in this work. From the measured times of flight and positions of impact of the ions, the mass-to-charge ratios and the three-dimensional momentum vectors were calculated. The two different protons $H1^+$ and $H2^+$ as well as the two oxygen ions $O1^+$ and $O2^+$ of the molecule [as enumerated in Fig. 1(a)] were distinguished using a procedure described in Ref. [6]. Here, H2 and O2 refer to the hydrogen and oxygen that are part of the hydroxyl group (OH). In the following, we present a subset of the data in which the three charged fragments C^+, $O2^+$, and $H2^+$ were detected. To quantify the degree of handedness of the excited molecule, a triple product of the three measured momentum vectors $\vec{k}_{H2^+}, \vec{k}_{O2^+}$, and $\vec{k}_{C^+}$ was calculated [6],

$$\cos\alpha = \frac{(\vec{k}_{O2^+} \times \vec{k}_{C^+}) \cdot \vec{k}_{H2^+}}{|\vec{k}_{O2^+} \times \vec{k}_{C^+}| \cdot |\vec{k}_{H2^+}|}. \quad (1)$$

Since heavy undetected fragments, which can be charged or neutral, also carry momentum, the three measured momenta $\vec{k}_{H2^+}$, $\vec{k}_{O2^+}$, and $\vec{k}_{C^+}$ are mostly noncoplanar, allowing the cosine of the chiral angle α in Eq. (1) to be nonzero.

Figure 2 shows our corresponding experimental results. In panel (a), we depict the measured distribution of $\cos\alpha$ [Eq. (1)] recorded at a photon energy of 288.2 eV, which corresponds to the C 1s $\rightarrow \pi^*$ excitation (blue curve), and a photon energy of 532.1 eV, which corresponds to the O 1s $\rightarrow \pi^*$ excitation (red curve). We employed circularly polarized light in both measurements. The two distributions show a double-peak structure with a slight minimum located at the planar configuration ($\cos\alpha = 0$). The peaks at $\cos\alpha = -0.3$ and $\cos\alpha = +0.3$ correspond to a breakup of left- and right-handed chiral geometries, i.e., of the S and R enantiomers of the molecule. The distribution measured for the C 1s $\rightarrow \pi^*$ resonance employing linearly polarized light for the excitation (green curve in the same panel) is similarly broad. The fact that it does not exhibit a clear minimum at $\cos\alpha = 0$ could be related to a considerably smaller experimental count rate and, thus, significantly larger statistical uncertainties, as compared to the measurements with circularly polarized light. Promoting the C 1s electron to a state of σ^* character (planar equilibrium structure) leads to a narrower distribution of $\cos\alpha$ with a local maximum at the planar breakup geometry [see Fig. 2(b)]. This finding indicates the ultrafast molecular bending of the excited molecule upon population of the π^* state during the lifetime of the 1s hole, i.e., in the time between the excitation and the multiple Auger-Meitner decays that spawn the Coulomb explosion. This

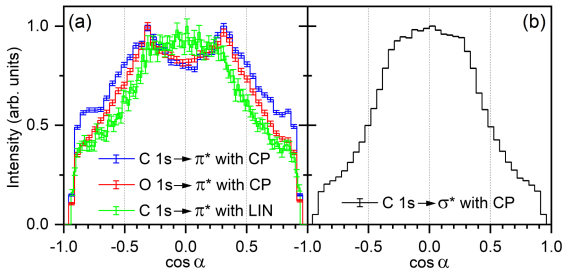

FIG. 2. Distributions of $\cos\alpha$ [Eq. (1)], integrated over all orientations of the molecule with respect to the light propagation direction. The value of $\cos\alpha = 0$ corresponds to planar molecular geometry, and $\cos\alpha > 0$ or $\cos\alpha < 0$ correspond to the nonplanar R or S enantiomeric configurations. (a) Fragmentation following C 1s $\rightarrow \pi^*$ excitation of formic acid at a photon energy of $E_\gamma = 288.2$ eV [10] with circularly polarized light (blue curve). Fragmentation following O 1s $\rightarrow \pi^*$ excitation at a photon energy of $E_\gamma = 532.1$ eV [10] with circularly polarized light (red curve). Fragmentation following C 1s $\rightarrow \pi^*$ excitation at a photon energy of $E_\gamma = 288.2$ eV [10] with linearly polarized light (green curve). (b) Distribution of $\cos\alpha$ after C 1s $\rightarrow \sigma^*$ excitation of formic acid at a photon energy of $E_\gamma = 296.1$ eV [10]. The error bars represent statistical uncertainties.

pyramidalization does not occur for molecules excited to σ^* states making their breakup more planar reflecting the fluctuations around the planar geometry. Most importantly, all distributions depicted in Fig. 2 have an expectation value $\langle\cos\alpha\rangle \approx 0$ showing that, as expected, even for the case where a pyramidalization into a chiral structure occurs, both enantiomers are produced with equal probability.

To demonstrate experimentally how this symmetry can be broken, we show in Fig. 3 the dependence of the expectation value $\langle\cos\alpha\rangle$ on the direction of impact of the exciting photon with respect to the molecule. For this, we define a molecular coordinate frame from the plane spanned by the C^+ and $O2^+$ momentum vectors. As the heavy fragments dominate the momentum balance, this plane approximates the molecular plane before the excitation. A sketch indicating the definition of the molecular frame and the angle of the photon impact direction is shown in Fig. 1(a). Accordingly, $\cos\theta = \pm 1$ corresponds to photons impinging approximately normally to the initial molecular plane. The color maps in Figs. 3(a)–3(e) showing the dependence of $\langle\cos\alpha\rangle$ on the photon propagation direction indicate values ranging between -0.2 and $+0.2$. This suggests that the direction of impact of the photon is a control parameter to achieve enantiomeric excess. To elucidate further the underlying mechanism causing the effect, we present in Figs. 3(a)–3(c) the results obtained using left- and right-handed circularly polarized and linearly polarized light. We do not find a significant influence of the light helicity on the shape of the measured $\langle\cos\alpha\rangle$ distribution (only the contrast is slightly lower in the case of linearly polarized light). We therefore conclude that the underling mechanism responsible for the enantiosensitive excitation does not rely on the interplay between electric- and magnetic-dipole transition moments, as is the case in pioneering theoretical work by Rouxel *et al.* [20]. There, the authors predict that the helicity of circularly polarized light, used for exciting randomly oriented formic acid molecules, directs which enantiomer is preferably formed in the excited state. On the contrary, the effect observed here disappears when integrating over the molecular orientation (as indicated by Fig. 2) and does not invert the preferred enantiomer upon inverting the light helicity. The present results agree with the previous study of a chiral fragmentation of the formic acid molecule [6], where an enantioselectivity of the pyramidalization was achieved by changing the direction from which a circularly polarized strong laser pulse encountered the molecule. The handedness of the pyramidalized molecule was mainly given by the direction of impact of the light, just as in our present study. In contrast, a much smaller additional light-helicity dependence was reported in Ref. [6], which is absent in our present results using one-photon excitation. We speculate that this slight helicity dependence observed in Ref. [6] was caused by additionally absorbed photons from the circularly polarized light pulse probing the excited chiral molecular configuration and driving the fragmentation process. In the present work, no additional photons are

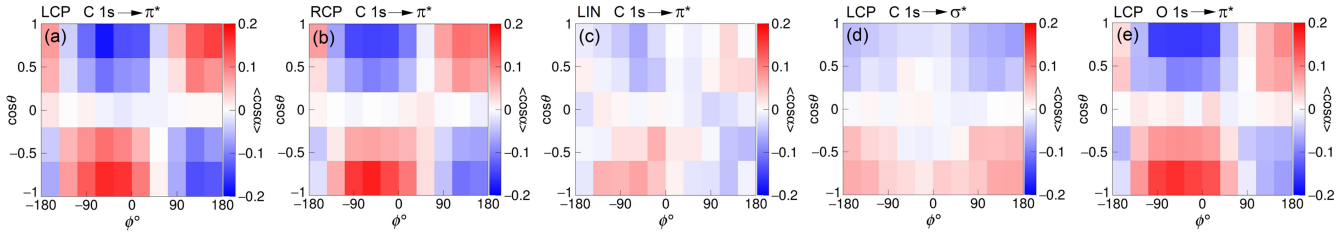

FIG. 3. Controlling enantiomeric excess with the photon propagation direction. (a)–(e) The color-coded $\langle\cos\alpha\rangle$ distributions as functions of the direction of light propagation as defined in Fig. 1(a). Positive values of $\langle\cos\alpha\rangle$ (in red color) correspond to a preferred excitation of the nonplanar R enantiomeric configuration, and negative (in blue) to the S. (a)–(c) Data for the photon energy of $E_\gamma = 288.2$ eV corresponding to the C 1s $\rightarrow \pi^*$ excitation using left circularly (a), right circularly (b), and linearly (c) polarized photons. (d) Same as in panel (a), but at $E_\gamma = 296.1$ eV, corresponding to the C 1s $\rightarrow \sigma^*$ excitation. Note that the range of the color bar is the same as in panels (a)–(c). (e) Same as in panel (a), but at $E_\gamma = 532.1$ eV, corresponding to the O 1s $\rightarrow \pi^*$ excitation.

absorbed, and the fragmentation is driven solely by molecular relaxation processes, including Auger decay. Finally, as already expected from Fig. 2(b), we do find a rather different and less significant effect for the excitation to the σ^* state [see Fig. 3(d)], as compared to the π^* state. Our finding, that the population of the π^* state is the decisive factor, is further confirmed by a measurement performed at a photon energy of 532.1 eV. At this energy, the same π^* orbital is resonantly populated by excitation from the O2 1s orbital [Fig. 3(e)]. We find the same general pattern, only the ϕ angle at which the effect changes sign has slightly moved from approximately $\phi = 50°$ to $\phi = 90°$. This is due to the different position of the initial $1s$ orbital in the molecule, which imprints an additional phase shift between excitation amplitudes [see Eq. (2) and respective discussion below].

We now discuss the physical mechanism controlling the direction of pyramidalization of the formic acid molecule and, thus, generating the different enantiomers. The electronic ground state of formic acid has a planar equilibrium configuration, i.e., the potential energy curve as function of a generalized bending coordinate Q has a local minimum at the planar configuration at $Q = 0$ and is symmetric. This is sketched in Fig. 1(b) by the lower potential energy curve. The ground-state nuclear wave function is schematically shown by a yellow Gaussian distribution. A planar molecule exists only for Q being exactly zero, and, for a given degree of the pyramidalization $|Q|$, there is an equal number of molecules with R and S enantiomeric configurations. This entails that any hypothetical experimental measurement of the configuration of a single molecule will always yield a chiral configuration, as the measure of the set of planar molecules is zero. Any planar, prochiral molecule thus exhibits dynamic chirality [21]. The π^* state in contrast is characterized by a double-well potential [upper potential energy curve in Fig. 1(b)] with minima at $Q < 0$ and $Q > 0$ (at the equilibrium positions, which correspond to the S and R enantiomers of the molecule). A vertical Franck-Condon transition from the ground to the excited electronic states produces the two enantiomers of the molecule depending on its initial configuration (i.e., Q) within the ground-state wave function at the instance of photoabsorption, as indicated in Fig. 1(b) by the vertical blue (for S) and red (for R) dotted arrows. Once excited and being on the left (or right) side of the barrier, subsequent molecular dynamics will yield a further increase of the molecule's bending until this motion along the excited-state potential energy surface is interrupted by the Auger decay.

The transition matrix element $M_q(Q, \theta, \phi)$ for the resonant population of the excited electronic state π^* depends on the molecular geometry (bending coordinate Q), the polarization of the absorbed light ($q = \pm 1$ for circular and $q = 0$ for linear polarization), and its propagation direction [given in the molecular frame of reference by the angles θ and ϕ as shown in Fig. 1(a)],

$$M_q(Q, \theta, \phi) = \sum_k \mathcal{D}^1_{kq}(\phi, \theta, 0) A_k(Q). \tag{2}$$

Here, $\mathcal{D}(\alpha, \beta, \gamma)$ is the Wigner matrix for a rotation over the three Euler angles, describing the orientation of the molecular frame in the laboratory. In the present case, they are defined as $\alpha = \phi$ and $\beta = \theta$, while the third angle γ can be chosen arbitrarily as its choice implies just a global phase on the total amplitude M_q. The quantities $A_k(Q)$ are the electric-dipole amplitudes for the $1s \rightarrow \pi^*$ excitation by either linear ($k = 0$) or circular ($k = \pm 1$) polarization, as given in the molecular frame of reference. They depend on the molecular geometry Q. The physical mechanism behind the symmetry breaking is the following: for given angles θ and ϕ from which the light impinges onto the molecule, the matrix element in Eq. (2) is different for positive and negative values of the bending coordinate Q, i.e., R or S enantiomeric configurations of the pyramidalized molecule are populated with different probabilities.

Figure 1(c) shows schematically the π^* orbital for the R configuration, where the H2 bond is artificially tilted upward ($Q > 0$) by $+20°$ out of the molecular plane. In this bent configuration, a larger fraction of the π^* density is located above the molecular plane. Note that the upper and lower side of a prochiral molecule are as distinguishable as the top and bottom side of the face of a clock. The initial C 1s orbital from which the electron is promoted is not centered with respect to the π^* orbital. The transition matrix element will maximize when the polarization vector points from the C center to the maximum of the π^* orbital. This intuitive expectation is confirmed by our calculation of the transition matrix element in Eq. (2) as a function of the angles θ and ϕ. Figures 4(a) and 4(b) illustrate how the handedness of the π^* excitation in the pyramidalized structures makes the excitation probability $|M_q(Q, \theta, \phi)|^2$ nontrivially dependent on these angles. The symmetry properties of the dipole amplitudes $A_{\pm 1}(Q) = A_{\pm 1}(-Q)$ and $A_0(Q) = -A_0(-Q)$ imply that the excitation probabilities of the two enantiomers in Figs. 4(a) and 4(b) are just shifted with respect to each other by an angle $\phi = 180°$.

Figure 4(c) shows the normalized difference between the computed excitation probabilities depicted in Figs. 4(a) and 4(b). This simple estimate of the enantiomeric excess yields features very similar to what we observe in the experiment [Figs. 3(b) and 3(b)], with the biggest surplus of R enantiomers located at $\theta = 180°$, $\phi = -30°$ and $\theta = 0°$, $\phi = 150°$, and with equal population of both enantiomers at $\theta = 90°$ and along the lines with $\phi = -120°$ and $\phi = 60°$. Since the calculations were performed at two fixed bending geometries of the molecule $Q = \pm 20°$, the theoretical contrast ranges in between ± 1, while it is expected to be somewhat smaller after dynamical averaging over the bending coordinate Q and binning in θ and ϕ angles, as inherent in the experiment. The qualitative agreement with the experiment indicates, however, the validity of the

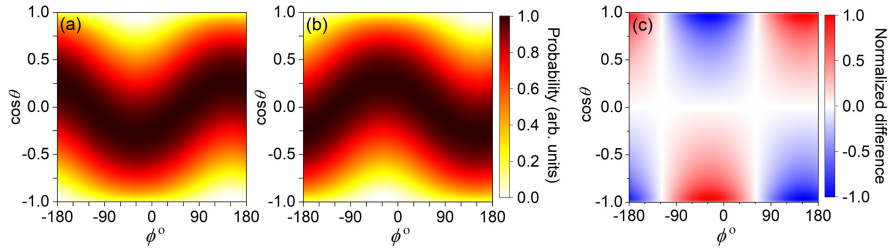

FIG. 4. Theoretical modeling of the symmetry breaking. (a) Excitation probability $\sigma^R = |M_{\pm1}(+20°, \theta, \phi)|^2$ for the vertical transition from the C 1s to the π^* orbital, shown in Fig. 1(c), as a function of the two angles θ and ϕ defining the light propagation direction, and (b) the same for its mirror image $\sigma^S = |M_{\pm1}(-20°, \theta, \phi)|^2$. (c) Normalized difference $(\sigma^R - \sigma^S)/(\sigma^R + \sigma^S)$.

proposed theoretical mechanism. Moreover, using the symmetry property of the dipole amplitudes $A_{-1}(Q) = -[A_{+1}(Q)]^*$, it is possible to show analytically that the matrix element in Eq. (2) obeys the following property: $M_{+1}(Q, \theta, \phi) = -[M_{-1}(Q, \theta, \phi)]^*$. This, in turn, explains the observed independence of the excitation probability $|M_q(Q, \theta, \phi)|^2$ from the handedness q of the incident light. Actually, in the electric-dipole approximation, switching the propagation direction of circularly polarized light is equivalent to switching its helicity. That is why, the color maps, shown in Figs. 3 and 4 for the $1s \rightarrow \pi^*$ excitation, do not change by a simultaneous transformation of $\cos(\theta) \rightarrow -\cos(\theta)$ (vertical flip) and $\phi \rightarrow \phi + 180°$ (horizontal shift). To summarize: chiral selectivity is achieved because the dipole matrix element between the transiently chiral ground state and the chiral excited state strongly depends on the propagation (or polarization) direction of the exciting photon in the molecular frame of reference.

We presented that enantioselectivity can be achieved without the need for a chiral precursor or chiral light. The symmetry breaking is imposed by the macroscopic experimental geometry itself. The prochiral molecule establishes a plane with a sense of rotation. Adding a noncoplanar vector to this plane, as given by the light propagation direction, establishes a coordinate frame of well-defined handedness. Such a coordinate frame is a necessary precondition for enantioselectivity [22]. We have demonstrated that resonant one-photon excitation under these geometric conditions can selectively drive the planar ground state of formic acid into a right- or left-handed chiral excited state. The enantioselectivity is achieved by fixing the light propagation direction in the molecular frame of reference. The effect is substantial, since it relies purely on the electric-dipole light-matter interaction, and it is expected to be general to all prochiral molecules.

Acknowledgments—This work was funded by the Deutsche Forschungsgemeinschaft (DFG)—Project No. 328961117—SFB 1319 ELCH (Extreme light for sensing and driving molecular chirality). The experimental setup was supported by BMBF. The calculations were supported in part through the Maxwell computational resources operated at DESY. F. T. acknowledges funding by the Deutsche Forschungsgemeinschaft (DFG, German Research Foundation)—Project 509471550, Emmy Noether Programme. J. B. W. acknowledges support from the National Sciences Foundation under Grant No. NSF-2208017. We acknowledge SOLEIL for provision of synchrotron radiation facilities and we would like to thank N. Jaouen and his team for assistance in using beamline SEXTANTS. We also acknowledge DESY (Hamburg, Germany), a member of the Helmholtz Association HGF, for the provision of experimental facilities. Parts of this research were carried out at PETRA III and we would like to thank M. Hoesch and his team for assistance in using beamline P04. Beam time was allocated for proposals H-20010092 and I-20200461.

[1] W. Kuhn and E. Knopf, Naturwissenschaften **18**, 183 (1930).
[2] D. Gerbasi, M. Shapiro, and P. Brumer, J. Chem. Phys. **124**, 074315 (2006).
[3] R. P. Cameron, S. M. Barrett, and A. M. Yao, New J. Phys. **16**, 013020 (2014).
[4] E. F. Thomas and N. E. Henriksen, J. Chem. Phys. **144**, 244307 (2016).
[5] A. Csehi, M. Kowalewski, G. J. Halász, and Á. Vibók, New J. Phys. **21**, 093040 (2019).
[6] K. Fehre, S. Eckart, M. Kunitski, M. Pitzer, S. Zeller, C. Janke, D. Trabert, J. Rist, M. Weller, A. Hartung, L. Ph. H. Schmidt, T. Jahnke, R. Berger, R. Dörner, and M. S. Schöffler, Sci. Adv. **5**, eaau7923 (2019).
[7] T. L. Ng and S. Bell, J. Mol. Spectrosc. **50**, 166 (1974).
[8] C. Fridh, J. Chem. Soc., Faraday Trans. 2 **74**, 190 (1978).
[9] L. M. Beaty-Travis, D. C. Moule, E. C. Lim, and R. H. Judge, J. Chem. Phys. **117**, 4831 (2002).
[10] I. Ishii and A. P. Hitchcock, J. Chem. Phys. **87**, 830 (1987).
[11] M. Pitzer *et al.*, ChemPhysChem **17**, 2465 (2016).
[12] M. Pitzer, G. Kastirke, Ph. Burzynski, M. Weller, D. Metz, J. Neff, M. Waitz, F. Trinter, L. Ph. H. Schmidt, J. B. Williams, T. Jahnke, H. Schmidt-Böcking, R. Berger, R. Dörner, and M. Schöffler, J. Phys. B **49**, 234001 (2016).
[13] J. Viefhaus, F. Scholz, S. Deinert, L. Glaser, M. Ilchen, J. Seltmann, P. Walter, and F. Siewert, Nucl. Instrum. Methods Phys. Res., Sect. A **710**, 151 (2013).

[14] M. Sacchi, N. Jaouen, H. Popescu, R. Gaudemer, J. M. Tonnerre, S. G. Chiuzbaian, C. F. Hague, A. Delmotte, J. M. Dubuisson, G. Cauchon, B. Lagarde, and F. Polack, J. Phys. Conf. Ser. **425**, 072018 (2013).
[15] K. Fehre, M. Pitzer, F. Trinter, R. Berger, A. Schießer, H. Schmidt-Böcking, R. Dörner, and M. S. Schöffler, Rev. Sci. Instrum. **92**, 023205 (2021).
[16] R. Dörner, V. Mergel, O. Jagutzki, L. Spielberger, J. Ullrich, R. Moshammer, and H. Schmidt-Böcking, Phys. Rep. **330**, 95 (2000).
[17] J. Ullrich, R. Moshammer, A. Dorn, R. Dörner, L. Ph. H. Schmidt, and H. Schmidt-Böcking, Rep. Prog. Phys. **66**, 1463 (2003).
[18] T. Jahnke, Th. Weber, T. Osipov, A. L. Landers, O. Jagutzki, L. Ph. H. Schmidt, C. L. Cocke, M. H. Prior, H. Schmidt-Böcking, and R. Dörner, J. Electron Spectrosc. Relat. Phenom. **141**, 229 (2004).
[19] O. Jagutzki, A. Cerezo, A. Czasch, R. Dörner, M. Hattaß, M. Huang, V. Mergel, U. Spillmann, K. Ullmann-Pfleger, Th. Weber, H. Schmidt-Böcking, and G. D. W. Smith, IEEE Trans. Nucl. Sci. **49**, 2477 (2002).
[20] J. R. Rouxel, M. Kowalewski, and S. Mukamel, Struct. Dyn. **4**, 044006 (2017).
[21] T. Kitamura, T. Nishide, H. Shiromaru, Y. Achiba, and N. Kobayashi, J. Chem. Phys. **115**, 5 (2001).
[22] A. Pier, K. Fehre, S. Grundmann, I. Vela-Perez, N. Strenger, M. Kircher, D. Tsitsonis, J. B. Williams, A. Senftleben, Th. Baumert, M. S. Schöffler, Ph. V. Demekhin, F. Trinter, T. Jahnke, and R. Dörner, Phys. Rev. Res. **2**, 033209 (2020).